



Ultrasound imaging of propagation of myocardial contraction for non-invasive identification of myocardial ischemia

Yuya Matsuno^{1*}, Hirofumi Taki^{1,2}, Hiroaki Yamamoto³, Michinori Hirano³, Susumu Morosawa³, Hiroaki Shimokawa³, and Hiroshi Kanai^{2,1*}

¹Graduate School of Biomedical Engineering, Tohoku University, Sendai 980-8579, Japan

²Graduate School of Engineering, Tohoku University, Sendai 980-8579, Japan

³Graduate School of Medicine, Tohoku University, Sendai 980-8574, Japan

*E-mail: kanai@ecei.tohoku.ac.jp

Received November 25, 2016; revised February 1, 2017; accepted February 20, 2017; published online June 6, 2017

Non-invasive identification of ischemic regions is important for diagnosis and treatment of myocardial infarction. In the present study, ultrasound measurement was applied to the interventricular septum of three open-chest swine hearts. The properties of the myocardial contraction response of the septum were compared between normal and acute ischemic conditions, where the acute ischemic condition of the septum originated from direct avascularization of the left anterior descending (LAD) coronary artery. The result showed that the contraction response propagated from the basal side to the apical side along the septum. The estimated propagation velocities in the normal and acute ischemic conditions were 3.6 and 1.9 m/s, respectively. This finding indicates that acute ischemia which occurred 5 s after the avascularization of the LAD promptly suppressed the propagation velocity through the ventricular septum to about half the normal velocity. It was suggested that the myocardial ischemic region could be identified using the difference in the propagation velocity of the myocardial response to contraction.

© 2017 The Japan Society of Applied Physics

1. Introduction

About 7.3 million people in the world, including 200,000 people in Japan, die from heart diseases every year.^{1,2)} The number of deaths due to heart diseases in Japan ranks second only to malignant neoplasm and accounts for 15.8% of annual deaths. Therefore, the prevention of heart diseases and their prompt and appropriate treatment are essential, and there is a compelling need for development of diagnostic methods that can be applied repeatedly and promptly with a high degree of accuracy.

Chest X-ray, computed tomography (CT),³⁾ magnetic resonance imaging (MRI),^{4,5)} and medical ultrasound are commonly used for the diagnosis of heart disease. Chest X-ray and CT are suitable to diagnose pathological conditions, but repetition is not recommended due to radiation exposure. Both morphological diagnosis by three-dimensional images and evaluation of coronary artery stenosis with contrast agents are possible with MRI; however, it cannot be applied to a patient with a cardiac pacemaker because MRI uses strong magnetic fields. In contrast, the use of ultrasound for diagnosis is suitable for repeated and prompt application because it is a non-invasive, low-cost, and real-time diagnostic method.^{6–10)}

Cardiac ischemia accounts for most heart diseases. Figure 1 shows an illustration of myocardial infarction. Myocardial ischemia originates from a decrease in blood flow caused by stenosis of a coronary artery. The prompt recovery of blood flow enables the ischemic region to avoid becoming necrotic, that is, becoming an infarct region. For myocardial ischemia, myocardial ischemia without pain (termed silent myocardial ischemia) is especially dangerous because it is difficult to detect.^{11,12)} Therefore, the development of a non-invasive, repeatedly applicable method of identifying a myocardial ischemic region would be very useful in the diagnosis and treatment of the early stage of myocardial infarction, that is, myocardial ischemia.

Several researchers have focused on myocardial ischemia.^{13–18)} Konofagou et al. reported that the propagation

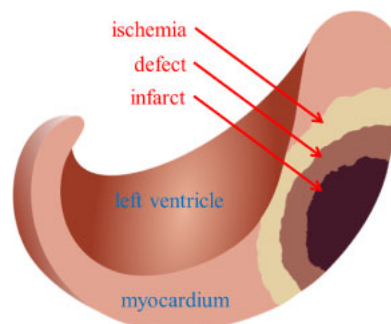


Fig. 1. (Color online) Outline of three layers separated by progression of myocardial infarction.

velocity of myocardial contraction in response to electrical stimulation decreases in the ischemic region of open-chest canine hearts,^{19,20)} and it has been found that the contraction response of the myocardium to electrical stimulation propagates at a speed of several meters per second.^{21–27)} Therefore, high temporal resolution is required for measurement of this response. However, the accuracy of in vivo measurement for the human heart is still low, and imaging of the relationship from the arrival of electrical stimulation to the myocardial contraction response is challenging.

In the present study, the propagation of the myocardial response to contraction along the interventricular septum (IVS) of an open-chest swine heart was measured with medical ultrasound to develop a method for identifying the ischemic region in the IVS. In the previous research, medium-sized hearts, such as canine and feline hearts, were mainly targeted,^{19,20)} whereas in the present study, swine hearts, whose circulatory construction function and size are similar to those of humans were used. Moreover, in the open-chest swine heart, the depth of the object (IVS) is shallow so that it is possible to keep a high frame rate to evaluate the myocardial contraction response with a high degree of accuracy. An ischemic condition was manually induced to compare the properties of the myocardial contraction

response at the septum between normal and ischemic conditions. Results confirmed that the ischemia promptly suppressed the propagation velocity in the IVS to about 70% of the normal condition or less at 5 s after the avascularization of the LAD.

2. Materials and methods

2.1 Measurement of myocardial micro vibration velocity

In the ultrasound measurement of the IVS of a swine heart, ultrasound pulses (center angular frequency $\omega_0 = 2\pi f_0$) are transmitted to the myocardium. The displacement of the myocardium at time t is calculated by the following equation:

$$x(t) = \frac{c_0 \tau(t)}{2}, \quad (1)$$

where c_0 is the velocity of ultrasound in soft biological tissue, and $\tau(t)$ is the round-trip propagation time of ultrasound between an ultrasonic probe and the myocardium.

When ultrasound pulses are transmitted at intervals of ΔT in a certain beam, the phase difference $\Delta\theta(x; t)$ between two succeeding received signals is given by

$$\begin{aligned} \Delta\theta\left(x; t + \frac{\Delta T}{2}\right) &= \theta(x; t + \Delta T) - \theta(x; t) \\ &= \frac{2\omega_0 \Delta x(t)}{c_0}, \end{aligned} \quad (2)$$

where $\Delta x(t)$ is the displacement of myocardium during the interval ΔT . Therefore, the minute vibration $v(x; t + \Delta T/2)$ during the interval ΔT at a depth x in the myocardium is obtained by

$$v\left(x; t + \frac{\Delta T}{2}\right) = \frac{c_0}{2\Delta T} \frac{\Delta\theta\left(x; t + \frac{\Delta T}{2}\right)}{\omega_0}. \quad (3)$$

In the present study, the phase difference at the center frequency f_0 was calculated by using the phased-tracking method,^{28,29)} and the minute vibration velocity $v_{ij}(t)$ was estimated at a j -th depth along the i -th ultrasonic beam at each time step.

2.2 Time delay measurement of myocardial contraction

In the present study, the vibration of the myocardium was measured as a waveform, which corresponds to myocardial contraction at various locations where the contraction is in response to the propagation of electrical stimulation. In order to visualize the propagation of the myocardial contraction response, the delay time τ_{ij} at a depth of j -th along the i -th ultrasonic beam was determined from the cross-correlation between the vibration velocity waveforms with large amplitude around the beginning of the ejection period. The width of the correlation window was set to be the same as the width of the vibration waveform and the search area was limited to before and after about 23 ms of the correlation window.

2.3 Propagation velocity estimation of myocardial contraction

In order to estimate the propagation velocity c_c of the contraction response in the IVS, the delay times $\{\tau_{ij}\}$ were averaged in the depth direction along the i -th ultrasound

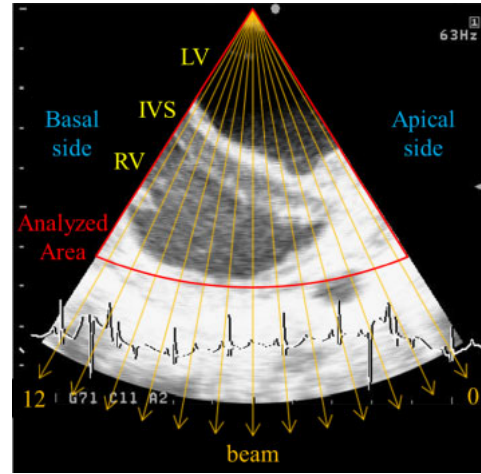


Fig. 2. (Color online) Conventional B-mode image obtained by ultrasound measurement in an open-chest swine heart. For the velocity measurement of Eq. (3) in the present study, sparse scanning was employed and the 13 selected ultrasonic beams (beam 0 to beam 12) are overlaid on the conventional B-mode image.

beam. The averaged delay time $\bar{\tau}_i$ along the i -th beam was obtained by the following operation:

$$\bar{\tau}_i = \frac{1}{N_i} \sum_{j=0}^{N_i-1} \tau_{ij}, \quad (4)$$

where N_i is the number of measurement points along the i -th ultrasound beam.

Next, the propagation velocity c_c was estimated by applying the weighted least-square method to the averaged delay time $\bar{\tau}_i$ along the i -th beam. The velocity within the region of interest was assumed to be constant and inverse of the standard deviation SD_i of the delay time along each ultrasound beam was employed as the weight. The power p of error was defined as follows:

$$p = \sum_{i=0}^{N-1} \frac{(\bar{\tau}_i - \alpha - \beta \cdot i)^2}{SD_i}. \quad (5)$$

After determining α and β to minimize p of Eq. (5), the propagation velocity c_c was estimated from the value of β .

2.4 In vivo experiments

Ultrasound diagnostic equipment (Aloka SSD-6500) with a probe having a center frequency of $f_0 = 3.75$ MHz was employed to acquire radio frequency (RF) data of the IVS in an open-chest swine heart. In this experiment, as shown in Fig. 2, the number of beams was restricted to 13 to maintain the frame rate $1/\Delta T$ at 429 Hz, the angle between successive beams was 5.6 degrees, and the sampling rate was 15 MHz. Beam 0 was set at the cardiac apical side. The reference position in the normal and ischemic conditions was set at a depth of 50 mm along beam 5.

The measurement process was as follows. First, as a control (normal condition) an ultrasound echo was acquired from the IVS in an open-chest swine heart (A), as shown in Fig. 3(a). Next, the blood flow of the left anterior descending (LAD) coronary artery was stopped manually to induce an acute ischemia condition at the IVS, and the same measurement as that applied to the normal condition was reapplied, as shown in Fig. 3(b). By analyzing these measurements, the propagation velocity was compared between normal and

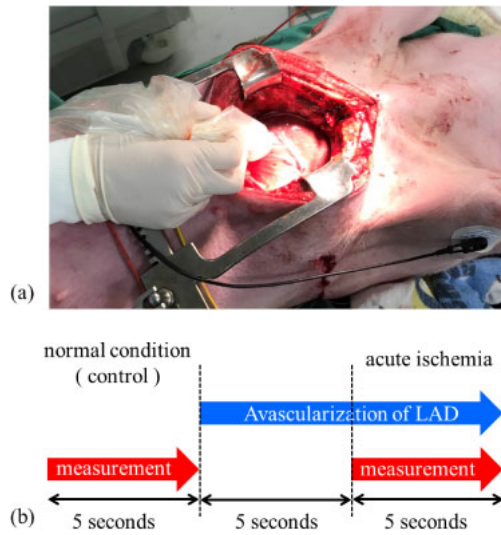


Fig. 3. (Color online) (a) Conditions of ultrasound echo measurement at interventricular septum in open-chest swine heart. (b) Protocol of measurement.

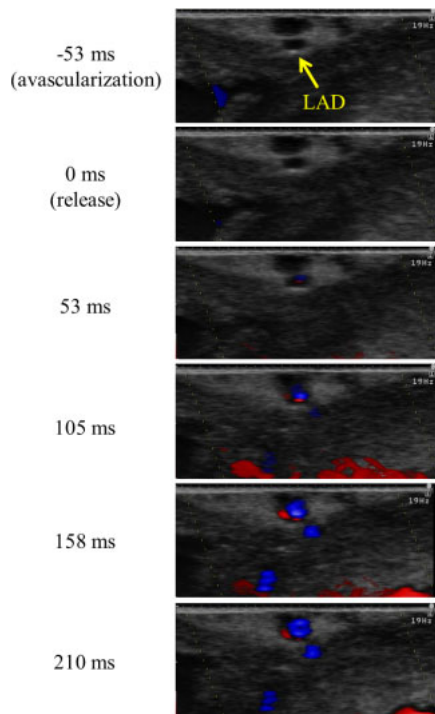


Fig. 4. (Color online) Color flow imaging of blood flow in the case of avasascularization by compressing the LAD with a finger and then releasing it.

ischemic conditions to visualize the change in propagation of the myocardial contraction response caused by the acute ischemic condition.

3. In vivo experimental results for swine hearts

The manual avasascularization of the LAD was confirmed by measurement of the blood flow therein. As shown in Fig. 4, the color flow image of the LAD was darkened during the period from -53 ms (avasascularization) to 0 ms (just released), when the blood flow of the LAD was stopped. A blue color then gradually appeared in the LAD from 53 ms after the release, showing an acute ischemic condition in the IVS.

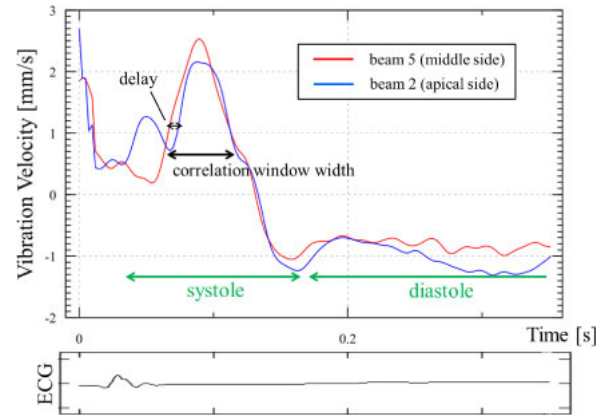


Fig. 5. (Color online) Minute vibration velocity waveform measured at the reference position (beam 5, depth 50 mm) and at another position (beam 2, depth 50 mm).

Figure 5 shows minute vibration velocity waveforms measured at the reference position (beam 5, depth 50 mm) and at a measurement position (beam 2, depth 50 mm) in the normal condition. The waveform of beam 2 (blue) was delayed from that of beam 5 (red), showing that the contraction response propagated from beam 5 (middle side) to beam 2 (apical side).

Figure 6 shows color maps of the amplitudes of the minute vibration velocity waveforms $\{v_{ij}(t)\}$ of 13 beams in the normal and ischemic conditions. In Fig. 6(c), for each beam, the velocity waveforms measured at 21 depths around the center point in the IVS along each beam, $\{v_{ij}(t)\}$ ($N_i/2 - 10 \leq j \leq N_i/2 + 10$), are shown, N_i being the number of measurement points along the i -th beam. At the beginning of the ejection phase just after the QRS waves, the peak times of the minute vibration velocity waveforms are delayed backward as the beam number becomes small, as shown in Fig. 6(a). On the other hand, as shown in Fig. 6(b), the delay in the ischemic condition was larger than that in the normal condition. These findings show that the contraction response propagates by a few m/s from the basal side to the apical side and that the propagation velocity decreases in the ischemic condition.

Figure 7 shows the delay time distribution $\{\tau_{ij}\}$ at each measurement point. The delay time increased from the basal side to the apical side in both the normal and ischemic conditions, showing propagation of contraction from the basal side to the apical side. The delay time difference from the basal side to the apical side in the normal condition was about 15 ms, and that in the ischemic condition was about 20 ms. Thus, myocardial acute ischemia promptly suppressed the propagation velocity of myocardial contraction.

Figure 8 shows the amplitude distribution of minute vibration velocity waveforms $\{v_{ij}(t)\}$ obtained at each measurement point superimposed on the B-mode image to confirm the estimation of the delay time distribution in Figs. 6 and 7. Each amplitude is shown by the maximum amplitude in the search area of the correlation window in Fig. 5. It was confirmed that the amplitude of the minute vibration velocity waveform was sufficiently larger than noise.

Figure 9 shows the average delay time $\{\bar{\tau}_i\}$ with respect to lateral distance x from beam 0. The solid line shows the straight line determined by applying the weighted least-

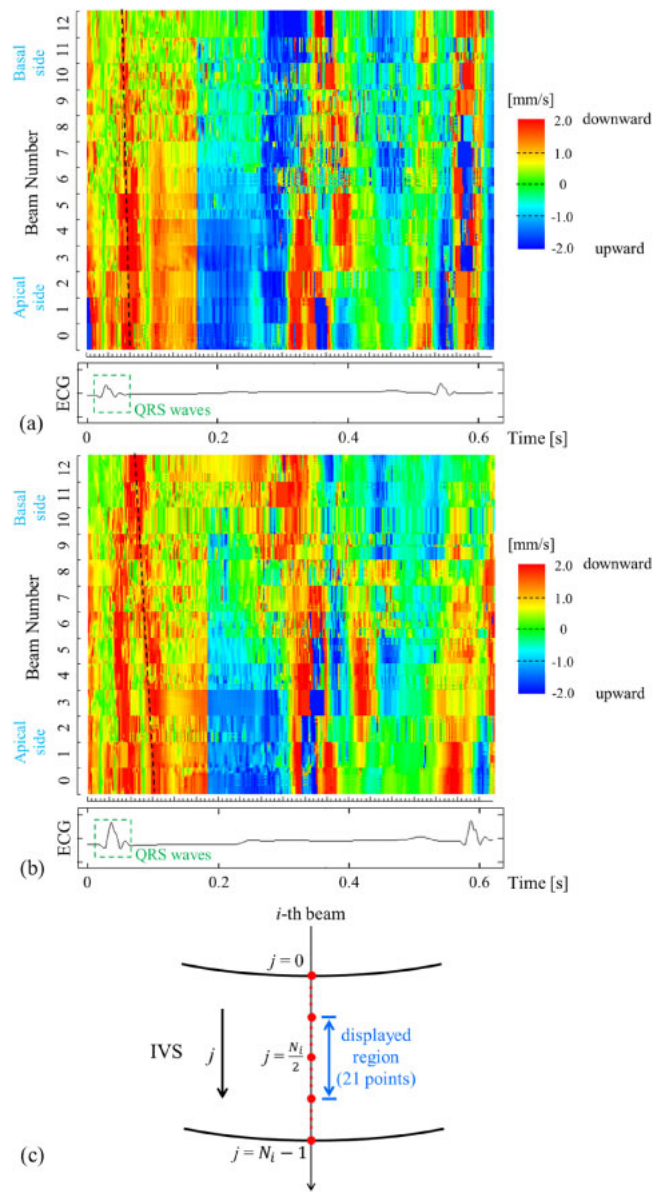


Fig. 6. (Color online) Temporal change of myocardial minute vibration velocity in 13 beams. Dotted lines show the delay of the peak times of the minute vibration velocity waveforms. (a) Normal (control), (b) ischemia, (c) outline of displayed region.

square method, as described in Sect. 2.3. As shown in Fig. 9, the propagation velocities in the normal and ischemic conditions were 3.6 and 1.9 m/s, respectively. These results show that the ischemia caused by the avascularization of the LAD promptly suppressed the propagation velocity along the IVS to about half the normal velocity. By applying the same measurement to two other swine hearts (B and C), the estimated propagation velocity values in the normal condition were 3.4 and 3.3 m/s, and for the ischemic condition the values were 2.0 and 2.4 m/s. These results show that the ischemia promptly suppresses the propagation velocity to about 70% of the normal condition or less.

In order to examine the influence on the propagation velocity of the myocardial contraction response while the ischemic condition continues, data for each beat during the avascularization for the swine heart (A) were compared. Figure 10 shows the transient response of the impaired propagation velocity due to ischemia. Each propagation

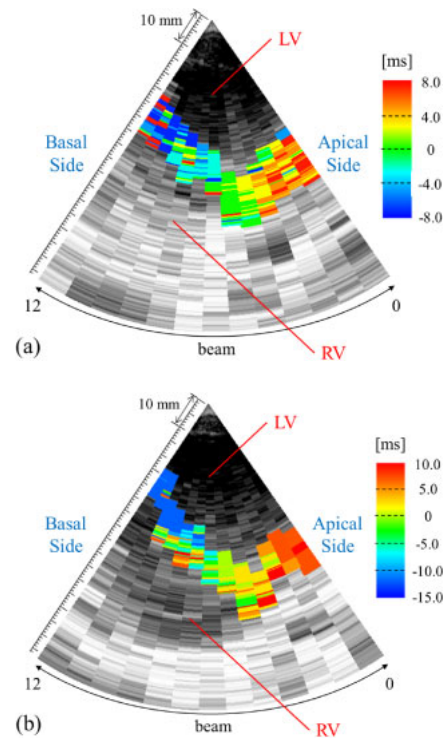


Fig. 7. (Color online) Delay time distribution of myocardial contraction response in (a) normal and (b) ischemic conditions.

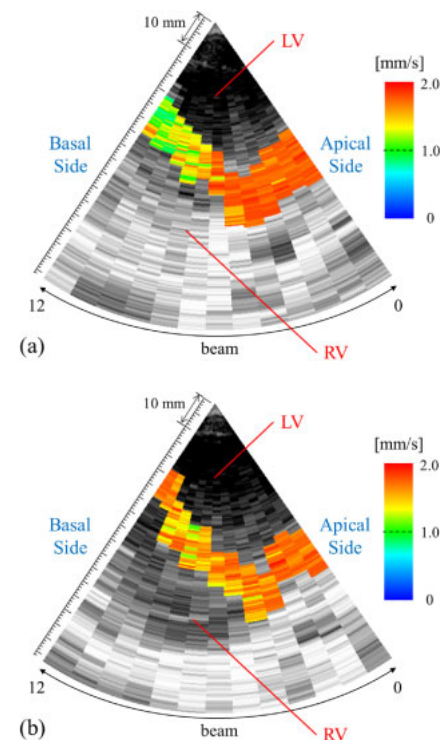


Fig. 8. (Color online) Amplitude distribution of minute vibration velocity waveform obtained for (a) normal and (b) ischemic conditions.

velocity for the period from the first beat to the fourth beat 5 s after the measurement for the normal condition gradually decreased from 1.90, 1.81, 1.76 to 1.69 m/s, respectively, as shown in Fig. 10(b). These results show that the progression of the ischemic condition suppressed the propagation velocity.

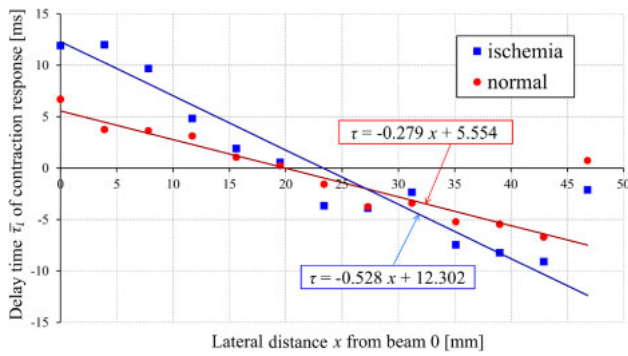


Fig. 9. (Color online) Approximate line estimated by the weighted least-square method considering the standard deviation in normal and ischemic conditions.

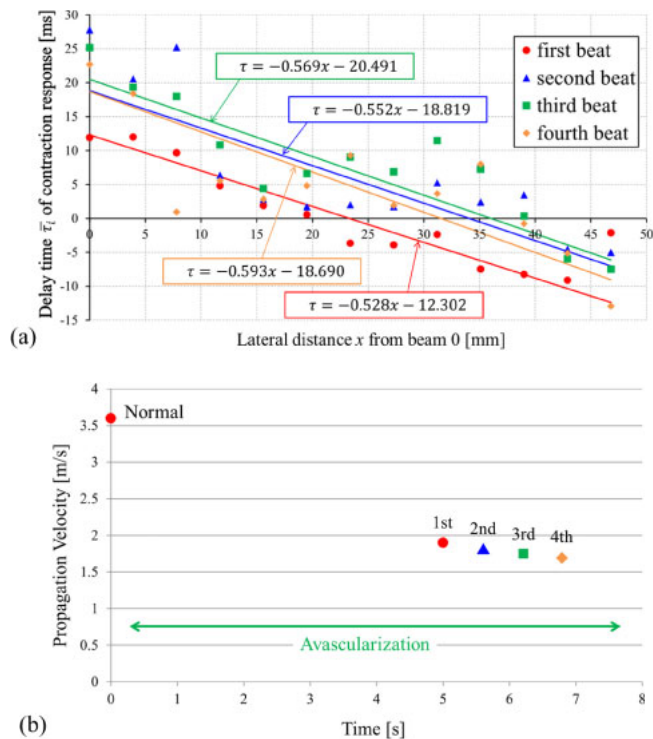


Fig. 10. (Color online) (a) Transient response of impaired propagation velocity due to ischemia. (b) Temporal change of the propagation velocity of myocardial contraction.

Since the procedure employed in the present study can easily produce ischemia, it will be helpful in elucidating not only the properties of myocardial contraction in normal and ischemic regions but also disease progression from the normal region to the ischemic region. The proposed method also has potential for use in non-invasive diagnosis of a region with reentry causing abnormal cardiac rhythm using the difference from the normal delay distribution and to evaluate the extent of the lesion quantitatively based on the difference of delay time between normal, ischemic and infarct regions.

4. Discussion

The myocardial minute vibration velocity shown after the QRS-wave of the electrocardiogram in Fig. 6(b) had bimodality in the ischemic condition. As shown in Fig. 11,

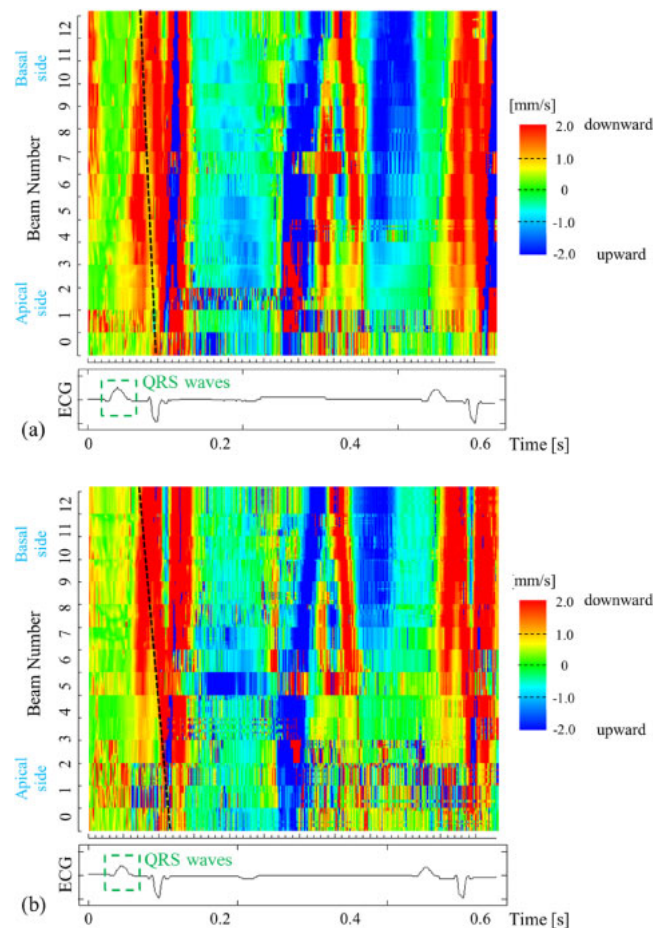


Fig. 11. (Color online) Temporal change of myocardial minute vibration velocity in another swine heart. Dotted lines show the delay of the peak times of the minute vibration velocity waveforms. (a) Normal and (b) ischemia.

similar results were obtained for another swine heart, but the cause of this phenomenon has not been ascertained and it is necessary to measure more swine hearts in the future.

The velocity amplitude of the apical side was larger than that of the basal side for the normal condition, as shown in Fig. 8(a). In the present study, the myocardial response to the arrival of the action potential rather than the propagation of the mechanical vibration along the IVS was measured. Moreover, since the beam direction and the IVS were not orthogonal at the basal side, the obtained velocity amplitude of the IVS was smaller than that on the apical side. On the other hand, the velocity amplitude of the basal side for the ischemic condition in Fig. 8(b) was larger than that in the normal condition. This is due to the difference in measurement position between the normal and ischemic conditions because the open-chest swine heart moves intensely. In the present study, the propagation of myocardial contraction was evaluated even when the amplitude at each position was different because only the delay in the propagation of the minute vibration velocity was considered.

In the ischemic myocardium, just after the time of coronary occlusion, it is known that the decrease of resting membrane potential (polarization failure) occurs because the concentration of potassium ions in the cell is decreased.³⁰⁾ Reduction of the resting membrane potential leads to the inactivation of the Na channel and the sodium current is reduced so that the upstroke of the action potential becomes slow. Therefore,

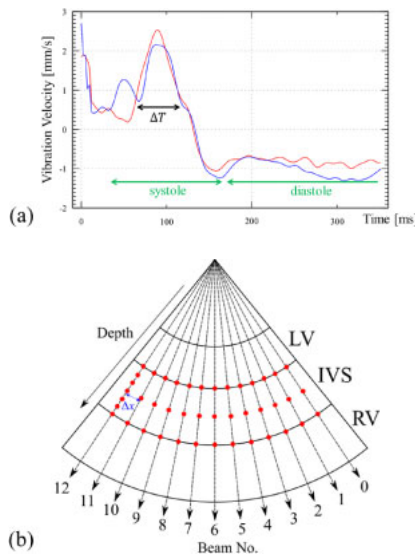


Fig. 12. (Color online) Two variables employed to calculate the wavelength λ_0 of the phenomenon to be measured. (a) ΔT ; period of the myocardial minute vibration and (b) Δx ; beam interval in the lateral direction at the middle level of the IVS.

the propagation velocity of myocardial contraction was decreased in the ischemic condition, as shown in Fig. 9.

In order to develop measurement technology as the basis of a method for identifying the ischemic region, the depth of the object (IVS) was shallow in this measurement. As shown in Fig. 12(a), the period ΔT of the minute vibration was about 50 ms, and the dominant frequency f_0 was about 20 Hz. Since the measured propagation velocity v of the myocardial contraction was estimated to be about 2 m/s, the wavelength λ_0 (mm) of the phenomenon was determined as

$$\lambda_0 = \frac{v}{f_0} \cong 100. \quad (6)$$

Since 13 beams were employed in the measurement, the beam interval Δx in the IVS was 4.0 mm, as shown in Fig. 12(b), which was much shorter than the wavelength λ_0 of the phenomenon to be measured. When the number of beams is reduced from 13 to 4, that is, only 0th, 4th, 8th, and 12th beams in Fig. 12(b) are selected and a sparser scan is performed, Δx is 12 mm, which is still sufficiently shorter than the wavelength λ_0 . Thus, the measurement with such sparse scanning is consistent for estimating the propagation velocity. Therefore, when applying the measurement to the human heart, it is possible to identify the myocardial ischemic region even if the number of beams is reduced to keep a high frame rate.

5. Conclusions

In the present study, the propagation of myocardial contraction along the IVS of open-chest swine hearts was measured by medical ultrasound. The properties of the myocardial contraction response in the IVS were compared between normal and acute ischemic conditions, where the acute ischemic condition of the IVS originated from the avascularization of the LAD. As a result, delay time distribution of the myocardial contraction response was visualized. These results show that the myocardial contraction response propagated from the basal side to the apical

side. In addition, the estimated propagation velocity values in the normal and ischemic conditions were 3.6 and 1.9 m/s, respectively. These results show that ischemia caused by avascularization of the LAD promptly suppresses the propagation velocity along the IVS to about half the normal velocity. By applying the same measurement to two other swine hearts, the estimated propagation velocity values in the normal condition were found to be 3.4 and 3.3 m/s, whereas those in the ischemic condition were 2.0 and 2.4 m/s. These results show that ischemia promptly suppresses the propagation velocity along the IVS to about 70% of the normal condition or less. Therefore, regarding myocardial contraction caused by acute ischemia, a prompt decrease in propagation velocity was confirmed by measurement and visualization in the present study.

- 1) S. Mendis, P. Puska, and B. Norrving, *Global Atlas on Cardiovascular Disease Prevention and Control* (World Health Organization, Geneva, 2011) p. 3.
- 2) Ministry of Health, Labour and Welfare, Report of Vital Statistics in 2012, p. 11.
- 3) L. T. Mahoney, W. Smith, M. P. Noel, M. Florentine, D. J. Skorton, and S. M. Collins, *Invest. Radiol.* **22**, 451 (1987).
- 4) L. Axel and L. Dougherty, *Radiology* **171**, 841 (1989).
- 5) M. B. Buchalter, J. L. Weiss, W. J. Rogers, E. A. Zerhouni, M. L. Weisfeldt, R. Beyar, and E. P. Shapiro, *Circulation* **81**, 1236 (1990).
- 6) G. R. Sutherland, G. D. Salvo, P. Claus, J. D'hooge, and B. Bijnens, *J. Am. Soc. Echocardiogr.* **17**, 788 (2004).
- 7) Y.-F. Cheung, *Nat. Rev. Cardiol.* **9**, 644 (2012).
- 8) Y. Sakai, H. Taki, and H. Kanai, *Jpn. J. Appl. Phys.* **55**, 07KF11 (2016).
- 9) Y. Kurokawa, H. Taki, S. Yashiro, K. Nagasawa, Y. Ishigaki, and H. Kanai, *Jpn. J. Appl. Phys.* **55**, 07KF12 (2016).
- 10) Y. Mochizuki, H. Taki, and H. Kanai, *Jpn. J. Appl. Phys.* **55**, 07KF13 (2016).
- 11) T. Kohya and H. Yasuda, *Jpn. Circ. J.* **56**, 1491 (1993).
- 12) F. J. Th. Wackers, L. H. Young, S. E. Inzucchi, D. A. Chyun, J. A. Davey, E. J. Barrett, R. Taillefer, S. D. Wittlin, G. V. Heller, N. Filipchuk, S. Engel, R. E. Rather, and A. E. Iskandrian, *Diabetes Care* (American Diabetes Association, Arlington, VA, 2004) p. 1954.
- 13) O. J. Elle, S. Halvorsen, M. G. Gulbrandsen, L. Aurdal, A. Bakken, E. Samset, H. Dugstad, and E. Fosse, *Physiol. Meas.* **26**, 429 (2005).
- 14) Z. Yang, H. Zhang, S. Kong, X. F. Yue, Y. B. Jin, J. Jin, and Y. C. Huang, *Physiol. Meas.* **28**, 481 (2007).
- 15) C. Tronstad, S. E. Pischke, L. Holhjem, T. I. Tonnessen, O. G. Martinsen, and S. Grimnes, *Physiol. Meas.* **31**, 1241 (2010).
- 16) W. N. Lee, J. Provost, K. Fujikura, J. Wang, and E. E. Konofagou, *Phys. Med. Biol.* **56**, 1155 (2011).
- 17) J. Provost, V. T. Nguyen, D. Legrand, S. Okrasinski, A. Costet, A. Gambhir, H. Garan, and E. E. Konofagou, *Phys. Med. Biol.* **56**, L1 (2011).
- 18) D. Romero, J. P. Martinez, P. Laguna, and E. Pueyo, *Physiol. Meas.* **37**, 1004 (2016).
- 19) J. F. Spann, R. A. Buccino, E. H. Sonnenblick, and E. Braunwald, *Circ. Res.* **21**, 341 (1967).
- 20) E. E. Konofagou, Proc. 28th IEEE EMBS Annu. Int. Conf., New York City, U.S.A., 2006.
- 21) D. Durrer, R. T. van Dam, G. E. Freud, M. J. Janse, F. L. Meuler, and R. C. Arzbaecher, *Circulation* **41**, 899 (1970).
- 22) H. Kanai, S. Yonechi, I. Susukida, Y. Koiwa, H. Kamada, and M. Tanaka, *Ultrasonics* **38**, 405 (2000).
- 23) A. M. Katz, *Physiology of the Heart PA* (Lippincott Williams & Wilkins, Philadelphia, PA, 2001) 3rd ed., p. 518.
- 24) H. Kanai and Y. Koiwa, *Ultrasound Med. Biol.* **27**, 481 (2001).
- 25) H. Kanai, *IEEE Trans. Ultrason. Ferroelectr. Freq. Control* **52**, 1931 (2005).
- 26) H. Kanai, *Ultrasound Med. Biol.* **35**, 936 (2009).
- 27) H. Kanai and M. Tanaka, *Jpn. J. Appl. Phys.* **50**, 07HA01 (2011).
- 28) H. Kanai, M. Sato, Y. Koiwa, and N. Chubachi, *IEEE Trans. Ultrason. Ferroelectr. Freq. Control* **43**, 791 (1996).
- 29) H. Kanai, H. Hasegawa, N. Chubachi, Y. Koiwa, and M. Tanaka, *IEEE Trans. Ultrason. Ferroelectr. Freq. Control* **44**, 752 (1997).
- 30) H. Iinuma, T. Yamashita, T. Fu, and K. Kato, *Heart* (Japan Heart Foundation, Tokyo, 2001) p. 340.